

Modeling zooplankton development using the monotonic upstream scheme for conservation laws

Nicholas R. Record* and Andrew J. Pershing

University of Maine School of Marine Sciences and the Gulf of Maine Research Institute, Portland, ME

Abstract

Numerical diffusion along the age/stage axis is recognized as a significant problem in the modeling of zooplankton populations in dynamic physical environments. We demonstrate the utility of borrowing schemes from numerical fluid dynamics to address this problem. In particular, we use the monotonic upstream scheme for conservation laws (MUSCL) to model the zooplankton *Calanus finmarchicus* in the Gulf of Maine. Applying this scheme to the molting term substantially reduces numerical diffusion without requiring the introduction of additional state variables. The improvement is on average equivalent to a 3- to 5-fold increase in the number of state variables, but without the run-time costs of such an increase. Basic strategies for assessing numerical schemes are discussed, and some consequences of numerical diffusion in the age domain are demonstrated.

Introduction

Coupling biological models with 2-D and 3-D circulation models has become a common and effective tool for understanding the dynamics of spatially heterogeneous populations in the ocean (Wroblewski 1982; Lynch et al. 1998; Gentleman 2002; Runge et al. 2004; Speirs et al. 2006). Biological systems are often modeled by a system of differential equations, so solving these systems numerically requires the same considerations as the numerical modeling of physical systems, including accuracy, stability, and convergence. In particular, numerical diffusion along the age axis or stage axis is recognized as a significant source of error in the modeling of zooplankton populations, resulting in early adulthood, and hence unrealistically early egg production, for a portion of the population (Davis 1984; Lynch et al. 1998; Runge et al. 2004). This type of numerical diffusion may be viewed as a smearing of the age structure or stage structure of a population. Various algorithms and strategies have been adopted to address this issue, includ-

ing well-resolved age classes (Davis 1984; Lynch et al. 1998; Zakardjian et al. 2003), individually based models (IBMs) (Batchelder et al. 2002; Runge et al. 2004), and dynamic time-step constraints (Gurney et al. 2001) to name a few, each with advantages and drawbacks. The issue of numerical diffusion is not new, and there exists a large body of literature on various numerical schemes designed to reduce or eliminate numerical diffusion in physical systems, especially fluids (Durran 1999; Wang and Hutter 2001). We demonstrate by example that these numerical schemes can be easily adapted to the modeling of zooplankton without the drawbacks that accompany alternative methods.

There are many advantages to using well-established numerical schemes to address the issue of numerical diffusion. Such schemes are easy to insert into a coded model without the need for additional state variables or additional constraints on time steps or age resolution. Because there is no loss of flexibility in the choice of temporal, spatial, and age resolution, the physical modeling need not be compromised, and any level of complexity in the age distribution may be preserved without additional cost. There is also a vast body of literature discussing the implementation of these schemes as well as strategies for dealing with error (Durran 1999). These numerical methods have often been developed for problems that are much more complex than life history models (Löhner 2001).

Here we present a numerical scheme that was highly effective for our modeling objectives: the monotonic upstream scheme for conservation laws (MUSCL) (van Leer 1979). This serves as an instructive example of the application of this type of numerical scheme to population modeling. The process of assessing the scheme also serves to highlight consequences of

*Corresponding author: E-mail: nrecord@gmri.org

Acknowledgments

This work benefited greatly from discussions with Jeffrey Runge and Dan Pendleton. Linda Woodard provided invaluable assistance with the advection-reaction-diffusion code. This study was supported by the National Science Foundation's Information Technology Research program (grant 0312610). Research was conducted in part using the resources of the Cornell University Center for Advanced Computing, which receives funding from Cornell University, New York State, the National Science Foundation, and other leading public agencies, foundations, and corporations.

numerical diffusion and to offer a strategy for assessing and comparing other solutions to this model.

We use “stage axis” interchangeably with “age axis” with the understanding that stage is not the only metric for age in life-history modeling. Depending on the species of interest, the modeler may choose another metric. The methods laid out in this article apply equally well to other metrics, as subdividing the population by length class, size class, or age class is mathematically equivalent.

Procedures

Modeling Calanus finmarchicus—We use as an example the copepod *Calanus finmarchicus* (henceforth *Calanus*), a dominant zooplankton in much of the North Atlantic, and an important prey for a diversity of species (Mauchline 1998). Typical of calanoid copepods, *Calanus* development includes 13 stages: egg, 6 naupliar stages (N1–N6), 5 copepodid stages (C1–C5), and adult (Mauchline 1998). In a 2-D biophysical coupled model (e.g., Lynch et al. 1998), *Calanus* concentrations are modeled using an advection-diffusion-reaction equation,

$$(1) \quad \frac{\partial \mathbf{c}}{\partial t} = -\mathbf{u} \cdot \nabla \mathbf{c} + \frac{1}{h} \nabla(kh \nabla \mathbf{c}) + R(\mathbf{c}, x, t),$$

where \mathbf{c} is the vector of *Calanus* stage concentrations at a point in space x and a time t , \mathbf{u} is the velocity of water, k is the diffusivity, h is the depth of the surface layer over which the model is integrated, and R is the reaction term that implements biology (reproduction, development, and mortality). The full formulation of the model is given in Appendix A. The advection and diffusion terms describe the physics of the environment. The reaction term R describes the biology, and must contain a molting term that models the development of *Calanus* through the 13 life stages. A molting scheme at some given spatial position x is expressed as follows:

$$(2) \quad \frac{\partial c}{\partial t} + \frac{\partial(gc)}{\partial s} = 0,$$

where $c(s, t)$ is the number of individuals in life stage s at time t , and $g(s)$ is the development rate, or molting rate, and may be dependent on external factors, such as temperature and food. It is in the molting term that numerical diffusion along the age axis appears. Equation (2) is equivalent to an advection equation, so strategies for reducing numerical diffusion in modeling the advection equation can be applied.

A brief review of numerical diffusion—To illustrate the issue of numerical diffusion, we will consider equation (2) as modeled using the upstream Eulerian scheme (also referred to as the “donor cell” scheme). This is a common scheme in biological modeling because of its simplicity and stability (reviewed by Runge et al. 2004). However, with a small number of life stages, i.e., a large Δs , or for a small time step Δt , there is typically a large amount of numerical diffusion. For now, we will assume a constant development rate g . The upstream Eulerian scheme is discretized as follows:

$$(3) \quad c_j^{n+1} = c_j^n - \frac{g\Delta t}{\Delta s} (c_j^n - c_{j-1}^n),$$

where superscripts indicate time step and subscripts indicate stage or age. Using Taylor expansions, a truncation error for this scheme can be expressed as follows:

$$(4) \quad \frac{\partial c}{\partial t} + g \frac{\partial c}{\partial s} = \frac{g\Delta s}{2} (1 - \nu) \frac{\partial^2 c}{\partial s^2} + H.O.T.$$

(*cf.* Odman 1997), where $\nu = g\Delta t/\Delta s$ is the Courant number and H.O.T. represents higher-order terms. Equation (4) is equivalent to the advection-diffusion equation up to high order, where the amount of numerical diffusion can be quantified using the value

$$D = \frac{g\Delta s}{2} (1 - \nu).$$

Note that when $\partial^2 c/\partial s^2$ is 0, numerical diffusion vanishes up to high-order terms. Thus the problem is most pronounced when the age distribution possesses abrupt jumps or discontinuities. Such a distribution is likely to occur in the event of a population bloom, or the physical mixing of water masses with different age distributions.

Stability for the upstream scheme requires that $0 \leq \nu \leq 1$, so that

$$(5) \quad 0 \leq D \leq \frac{g\Delta s}{2}.$$

The minimum diffusion occurs when $\nu = 1$. Given a stage-dependent development rate g , diffusion can be minimized by choosing either the maximum time step $\Delta t = \Delta s/g$ or the minimum stage step $\Delta s = g\Delta t$.

The modeling of *Calanus* often uses stage-dependent development rates based on laboratory experiments. Given a stage-dependent development rate (e.g., Davis 1984; Lynch et al. 1998; Zakardjian et al. 2003) and a Δt fixed by the physical circulation model, it may be possible to subdivide each of the 13 life stages to achieve an optimal Δs for each life stage. If development rate varies with environmental factors, such as temperature, choice of Δs is more limited.

If, on the other hand, the number of life stages is fixed, it is possible to minimize numerical diffusion by a prudent choice of Δt . For example, a characteristic generation length for *Calanus* at optimal temperatures is 30–40 days. If the life history is subdivided into the typical 13 development stages, then a time step of ~3 days will nearly eliminate numerical diffusion. If only 4 development stages are used (egg, naupliar, copepodite, adult), then a time step of ~8–10 days will nearly eliminate numerical diffusion. This time step, however, is greater than phytoplankton turnover rates, and phytoplankton blooms that are critical to modeling of *Calanus* could be missed.

Performing this sort of accuracy and stability analysis on higher-order schemes like the MUSCL is possible but much more complex. For schemes that do not yield so convenient an analysis, numerical tests may be run to determine optimal resolution.

As physical models improve in their ability to capture fine-scale complexity, there is often the associated requirement for a very small time step. In such cases, for the biological model to fully take advantage of this temporal-spatial complexity, the only option under the upstream differencing scheme is to

adopt an appropriately small Δs , which increases the number of state variables. Choosing Δs is thus a trade-off of high numerical diffusion versus slow run time and high memory usage. To avoid the unreasonably high number of state variables associated with a small Δs , population modelers have developed creative algorithms to deal with numerical diffusion. With very small populations, it is possible to use IBMs, where the specific state and spatial position of each individual is modeled (Batchelder et al. 2002). For larger populations, where it is too calculation-intensive to track every individual, Lagrangian ensemble models have been shown to be successful over short time periods (Carlotti and Wolf 1998). Such models replace the individual in IBMs with a meta-individual representing a subpopulation. Other models employ a different strategy, imposing dynamic constraints on Δt , essentially to optimize the Courant number as the model evolves (Ayati 2000; Gurney et al. 2001). This strategy is effective in reducing numerical diffusion but restricts flexibility in the physical model, in particular with respect to the choice of time step, and would be difficult to couple to biogeochemical models.

For populations without a spatial component, methods that track the mean state of individuals within a cohort have been shown to be effective under certain conditions. The escalator boxcar train (EBT) algorithm generalizes this approach, allowing mean-states for any number of variables, such as age, stage, length, or weight (de Roos 1988). Generally, just one state variable is used, such as mean size (de Roos et al. 1992) or mean age (Hu et al. in press), but the approach is generalized to allow for multiple state variables (Rinke and Vijverberg 2005; de Roos 1988; de Roos and Metz 1991). These methods are effective when age and spatial structure closely approximate a normal distribution, but they introduce new forms of numerical diffusion in cases where discontinuities in age or spatial distribution are present, such as is common in the presence of frontal gradients, tidal currents, mixing of cohorts, or development rates not constant along spatial axes.

It is important to note that, despite the drawbacks associated with high run time, the approach of using a large number of substages (i.e., small Δs) has advantages in addition to the reduction of numerical diffusion. First, the code is simple and allows the user to control the tradeoff between accuracy and speed. Second, the age structure of the population is more finely resolved. This is important in 2-D and 3-D models where advection may cause the physical mixing of differing age distributions, resulting in a more complex age distribution. This strategy should not be disregarded, as increasing processor speed will presumably greatly reduce the drawbacks associated with high run time.

Strategies borrowed from the modeling of physical systems can be employed without the drawbacks of the above methods, while maintaining many of the advantages of a substage approach. We use the MUSCL as one example among many possible numerical schemes that can be used to address the

problem of numerical diffusion.

The MUSCL—We implement the MUSCL in a simplified 0-D population model, as well as in a full 2-D biophysical coupled model. Small time steps are used throughout to magnify the potential effects of numerical diffusion, and to thereby better assess the methods. Effectiveness of the scheme is determined by calculating an error that compares model output to either the analytical solution (when possible) or the output of simulations that use very high-stage resolution. In other words, numerical diffusion is quantified by calculating the error as

$$(6) \quad Error = \frac{\sum |c_{best} - c|}{\sum |c_{best}|},$$

where sums may be taken over the spatial domain, the time domain, the stage domain, or multiple domains; c_{best} is either the exact analytical solution (when available) or the output of a very-high-resolution simulation.

Our choice of numerical scheme is driven by the objective of reducing numerical diffusion. The scheme is total variation diminishing (TVD) and drastically reduces numerical diffusion without introducing additional state variables. The superb flux limiter was chosen to minimize numerical diffusion, although other TVD flux limiters were seen to be nearly as effective. We have also found flux corrected transport (FCT) with high-order schemes such as the quadratic upstream interpolation for convective kinematics (QUICK) to be highly effective. For a thorough description and treatment of various numerical schemes, as well as instructions on implementation, we refer the reader to the literature (Durran 1999; Wang and Hutter 2001).

Briefly, TVD algorithms are those that constrain the sum over the domain of variation to be non-increasing. This prevents the development of spurious numerical oscillations and is accomplished by using a flux limiter. The method may be second- or third-order accurate where the solution is smooth, and it is first-order accurate where there are discontinuities or abrupt jumps. Details are given in Appendix B.

Assessment

Zero-dimensional test—We evaluated the effectiveness of the MUSCL through examples of increasing complexity, beginning with the case of a 0-D physical environment, constant development rate, and zero mortality. The population is initialized with a cohort of eggs, and zero everywhere else, analogous to the so-called pigpen test of numerical schemes. This case yields an analytical solution for c at any time t , so the error caused by numerical diffusion can be precisely determined by using the exact solution as c_{best} in equation (6).

The effects of numerical diffusion can be seen in a snapshot of the model outputs (Fig. 1A). Here $\Delta t = 1000$ s ($v \approx 0.6$), and the 13 *Calanus* life stages are subdivided into 10 substages each, so there are a total of 130 substages. This snapshot illustrates that the standard upstream solution, even with more than 100 substages, still yields a great deal of numerical diffusion using

this time step. The effectiveness of the MUSCL was assessed by calculating the normalized error, according to equation (6), at various resolutions and comparing to the same error calculated for the Euler upstream method (Fig. 1B). Sums in equation (6) were taken over the time and stage domains. The MUSCL output, with the same number of state variables, drastically reduces the numerical diffusion. In fact, with just 3 substages per life stage (39 total stages), the MUSCL exhibits less numerical diffusion than a 200+-stage Euler upstream scheme.

Simplified two-dimensional advection-diffusion-reaction test—Here, we elaborated on our first example by inserting the *Calanus* population into 2-D, depth-integrated circulation fields of the Gulf of Maine (Naimie 1996). The model was initialized with a cohort of eggs in the eastern Gulf of Maine that age to adulthood, advect, and diffuse throughout the model domain (Appendix A; Fig. 2). We introduced a stage-dependent development rate (Table 1). Temperature and chlorophyll were constant, and egg production was set to zero. We use $\Delta t = 1200$ s. The Courant number was variable, with a minimum of 0.019.

We calculated the error with respect to the stage-time distribution and the timing of adulthood. It is prudent to consider error in different domains when assessing a new numerical scheme, because there are cases where error is localized in one domain and may not be fully understood if sums are taken over all domains. Whereas it is certainly possible to carry out a more thorough error analysis than that presented here, for the purposes of this article, we focused on the most illustrative ways of analyzing the model output. In general, error in the spatial domain is also of interest. Because of the

uniformity of the model forcing (i.e., temperature and chlorophyll) in this example, the error in the spatial domain is negligible (this is not the case in a dynamic environment, as in the final example).

With this simplified modeling configuration, development rates do not vary in space, so an analytical solution could be calculated for the mean over the spatial domain. This allowed for precise error analysis over the time and stage domains. We first calculated an error analogous to that in our first example. The model output was averaged over the spatial domain, and sums in equation (6) were taken over the time and stage domains. A snapshot of the model outputs, for the 65 stage runs, illustrates the effects of numerical diffusion (Fig. 3A). In the exact solution, the population was concentrated in the C2 stage. The MUSCL solution exhibited some diffusion of the population into the C1 stage, whereas in the Euler upstream solution, the population stage structure was smeared across stages N5 to C4. The MUSCL output showed a drastic improvement over the Euler upstream scheme, although with some notable differences from the 0-D case. First, with only 13 substages, the MUSCL performed slightly worse than the Euler upstream scheme (Fig. 3B). Second, for runs with 1300 substages or more, numerical instabilities occurred. For the Euler upstream scheme, they occurred because the Courant number exceeded 1 for some portion of the population owing to the extremely high resolution, thereby introducing numerical instability. The MUSCL behaved similarly: if the stage resolution became too fine without appropriate adjustments to the time step, numerical instabilities occurred.

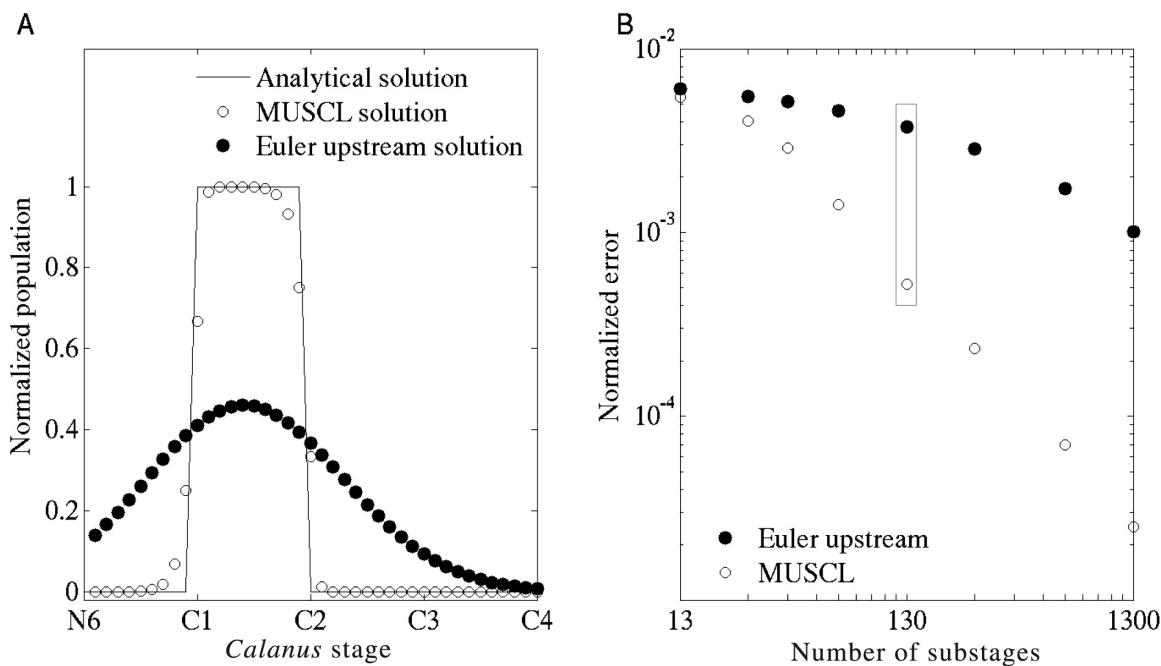


Fig. 1. A snapshot of the 0-D modeled population's stage distribution using a resolution of 130 substages for both the Euler upstream scheme and the MUSCL (A). Normalized error in the model output at various stage resolutions for both the Euler upstream scheme and the MUSCL (B). Box in (B) indicates the run that is shown in (A).

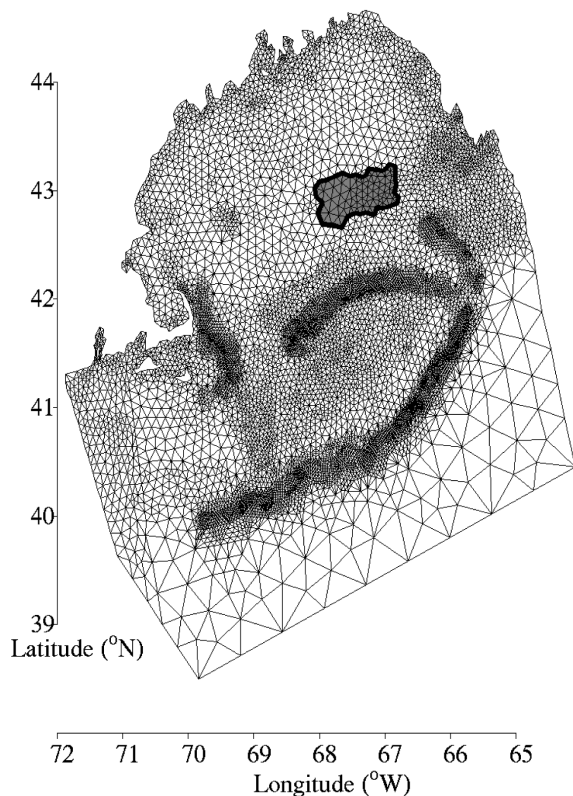


Fig. 2. Map of the Gulf of Maine showing the mesh that is the model's spatial domain. Highlighted region shows the location of the cohort of eggs at the initial time step.

Many of the high-resolution runs using the MUSCL performed better than the highest-resolution Euler upstream scheme. This can pose a problem in error analysis when no analytical solution is available. If error is determined by comparison to a high-resolution "best run," inaccurately high

errors will appear when a new method is actually performing better than the best run. This highlights the importance of assessing numerical methods in simplified cases for which exact solutions can be calculated.

Next we considered the timing of adulthood, which is one of the major concerns of numerical diffusion, as it controls generation time and thus population growth. The analytical solution provided an exact timing for reaching adulthood (Fig. 3C). For error calculation, we used the model output for the adult stage only, averaged over the spatial domain, and sums in equation (6) were taken over the time domain. A similar pattern appeared: the MUSCL showed drastic improvement over the Euler upstream scheme, with numerical instability occurring when there were more than 1000 substages (Fig. 3D). It is worth noting that although the Euler upstream scheme generally had a significantly higher error, the median timing of adulthood was equal to the timing provided by the exact solution, whereas the median timing of the MUSCL solution was slightly delayed. This source of error is small compared with that of numerical diffusion.

Full two-dimensional model test—Here we tested the full 2-D model by introducing a stage-dependent mortality rate (Table 1), a temperature-dependent mortality rate (Appendix A), and variable temperature and chlorophyll fields approximated from 2006 satellite data over the Gulf of Maine. Sea surface temperature and chlorophyll satellite data were obtained from the Ocean Color Web (Feldman and McClain 2007) and were collected by the MODIS-Aqua instrument. We also included egg production, because second-generation effects are a primary concern of stage diffusion and early adulthood. Because of the variable environment, the Courant number varied substantially, with a minimum value of 0.004.

Similar error analyses were performed as for the simplified 2-D case, as well as an analysis of error in the spatial domain.

Table 1. Stage-dependent parameter values.

| Stage | Index j | Behrdelek α_j | Mortality ϕ_j , day ⁻¹ | llev b_j | Dry Weight w_j , μg |
|--------|-----------|----------------------|--|----------------------|----------------------------------|
| Egg | 0 | 595 | 0.182 | 0.0329 | 0.50 |
| N1 | 1 | 388 | 0.336 | 0.0329 | 0.33 |
| N2 | 2 | 581 | 0.336 | 0.0329 | 0.49 |
| N3 | 3 | 1387 | 0.149 | 0.0329 | 1.0 |
| N4 | 4 | 759 | 0.026 | 0.0329 | 1.5 |
| N5 | 5 | 716 | 0.026 | 0.0329 | 2.1 |
| N6 | 6 | 841 | 0.026 | 0.0329 | 2.8 |
| C1 | 7 | 966 | 0.015 | 0.0333 | 4.2 |
| C2 | 8 | 1137 | 0.015 | 0.0333 | 13 |
| C3 | 9 | 1428 | 0.020 | 0.0333 | 23 |
| C4 | 10 | 2166 | 0.020 | 0.0333 | 64 |
| C5 | 11 | 4083 | 0.150 | 0.0333 | 170 |
| Adult | 12 | | 0.010 | | 276 |
| Source | | Lynch et al. 1998 | Eiane et al. 2002 | Campbell et al. 2001 | Speirs et al. 2006 |

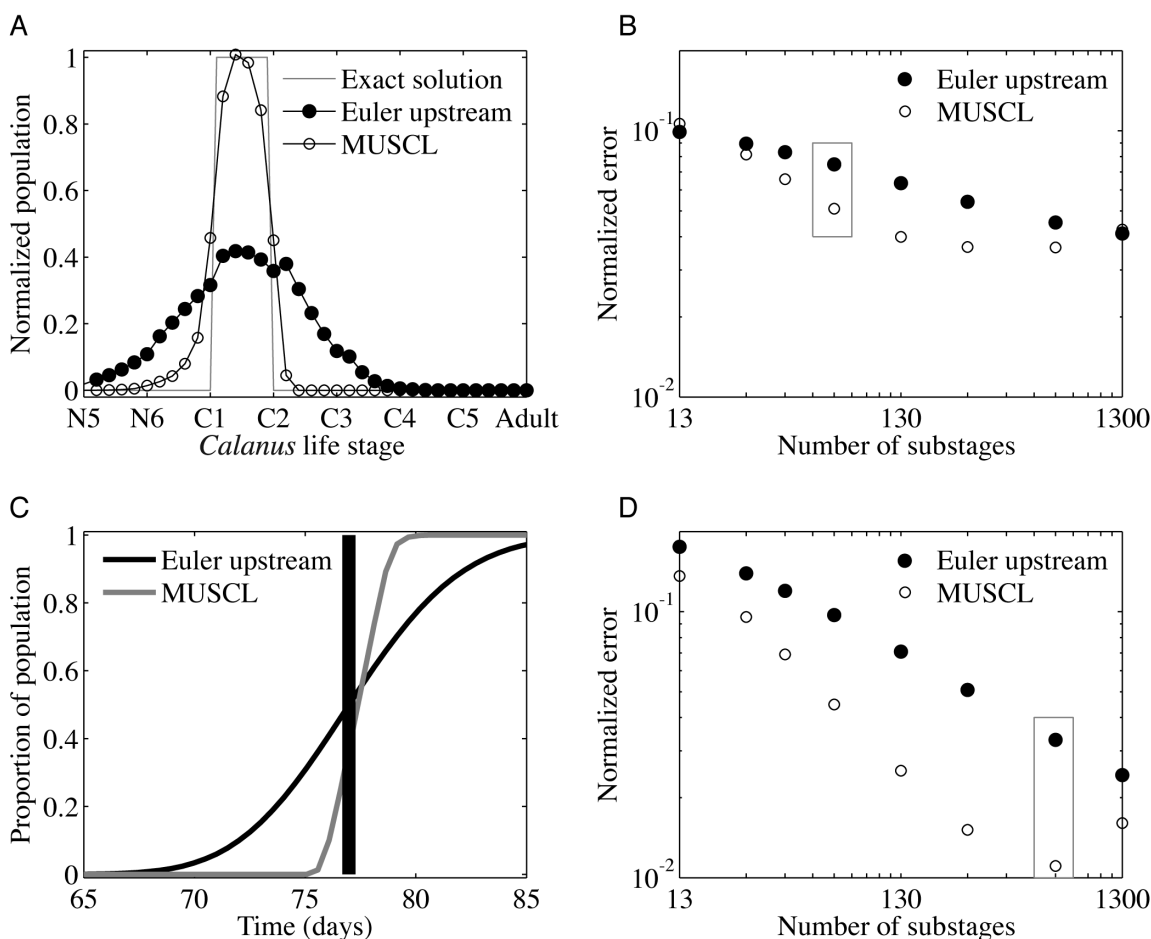


Fig. 3. A snapshot of the 2-D modeled population's stage distribution using a resolution of 65 stages for both the Euler upstream scheme and the MUSCL on day 32 (A). Normalized error in the model output over the time and stage domains at various stage resolutions for both the Euler upstream scheme and the MUSCL (B). A time series of the abundance of adults using 650 stages (C); vertical line shows the time at which the cohort should reach adulthood according to the analytical solution. Normalized error in the model output over the time domain for the adult stage at various stage resolutions for both the Euler upstream scheme and the MUSCL (D). Boxes in (B) and (D) indicate the runs that are shown in (A) and (C), respectively.

Again the MUSCL yielded as much improvement as an approximately 3- to 5-fold increase in the number of stages (Fig. 4B, D). The effects of numerical diffusion were most pronounced in egg production. With just a 13-substage Eulerian scheme, the second generation reached an abundance of 10–20 times what it should reach according to a well-resolved Eulerian scheme (Fig. 4C). Such an overcalculation would presumably have important consequences for any modeling exercise in which the second generation is of any interest.

Because the environment varies in space and time, an analytical solution is unattainable in all domains. We used a 650-stage Eulerian run as C_{best} since finer stage resolution generated numerical instabilities. This is somewhat problematic because our previous tests showed that at 130 substages, the MUSCL method performed better than a 650-stage Eulerian scheme (Fig. 3B, D). This was also apparent in a snapshot of the full model runs (Fig. 4A). If the MUSCL output were

compared with an inferior solution, the resulting error would be unrepresentatively high. Error calculations for the MUSCL at resolutions better than 130 stages are therefore unreliable.

With the introduction of spatially variable growth and mortality, the error calculated in the spatial domain followed a pattern similar to that of the error calculated in other domains (Fig. 4E, F). In the Eulerian scheme, this error was greater at day 120 than at day 60. Using the MUSCL, the error did not accumulate between days 60 and 120. The spatial effect of using the MUSCL method at various stage resolutions can be seen by viewing snapshots of the spatial distribution (Fig. 5). In this snapshot, there are two spatially distinct groups that have resulted from a flow bifurcation. One of these groups is not modeled at all in the low-resolution Eulerian scheme (Fig. 5A). Using the MUSCL, a much more moderate increase in stage resolution was sufficient to achieve a highly accurate spatial distribution, even in bifurcating flow fields.

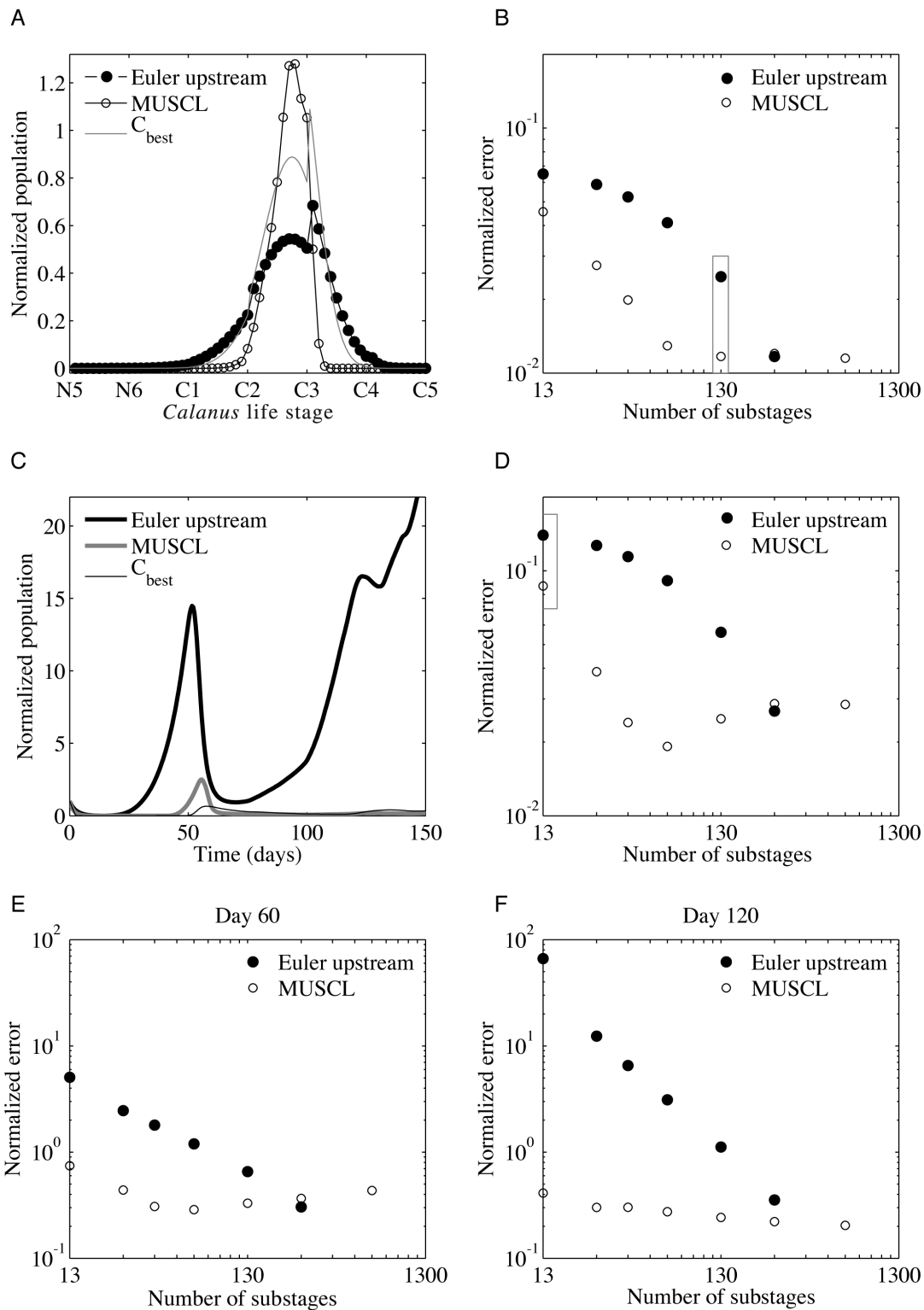


Fig. 4. A snapshot of the 2-D modeled population's stage distribution using a resolution of 130 stages for both the Euler upstream scheme and the MUSCL on day 32 (A). Normalized error in the model output over the time and stage domains at various stage resolutions for both the Euler upstream scheme and the MUSCL (B). A time series of the abundance of eggs using a resolution of 13 stages for both the Euler upstream scheme and the MUSCL (C); C_{best} uses 650 stages. Normalized error in the model output over the time domain for the egg stage at various stage resolutions for both the Euler upstream scheme and the MUSCL (D). Normalized error in the model output over the spatial domain on day 60 (E) and day 120 (F) at various stage resolutions for both the Euler upstream scheme and the MUSCL. Boxes in (B) and (D) indicate the runs that are shown in (A) and (C), respectively.

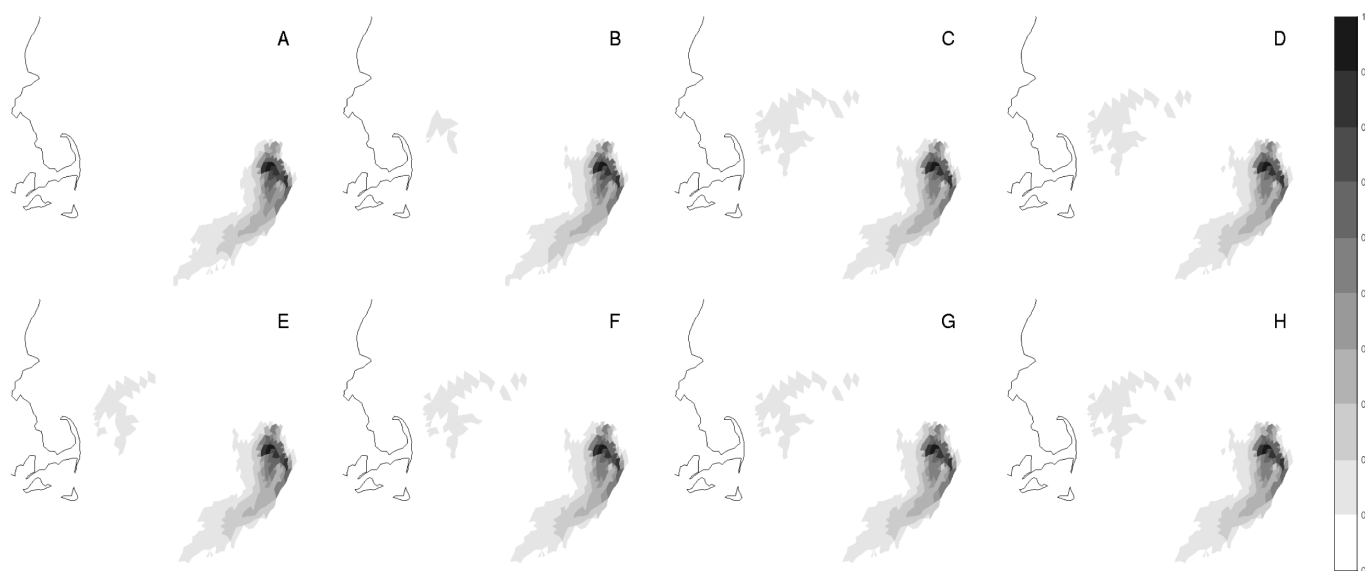


Fig. 5. A snapshot at day 100 of the spatial distribution at various stage resolutions for the Euler upstream scheme (A–D) and the MUSCL (E–H). Stage resolutions are 13 stages (A, E), 65 stages (B, F), 130 stages (C, G), and 650 stages (D, H). The color bar gives the normalized abundance value.

Discussion

The high computational cost of extending biological models into 2-D and 3-D space often limits the biological model itself to the simplest formulation (Runge et al. 2004). The MUSCL numerical method with the superbee flux limiter is seen here to greatly reduce numerical diffusion along the age axis without the introduction of additional state variables or of constraints on Δt or Δs . This is provided as one example of the application of well-established numerical methods to the problem of age diffusion. Other TVD methods and FCT methods can be effective as well, and an appropriate choice depends on the constraints and particulars of the physical and biological models as well as the ultimate goals of the modeling exercise.

Using the MUSCL in place of the Euler upstream scheme accomplishes an increase in accuracy equivalent to a 3- to 5-fold increase in the number of substages, but without the added cost of additional state variables. For modeling experiments on the scale of that demonstrated here, current processor speeds allow for a practical choice of 13 to 650 total stages, a range in which the advantages of the MUSCL are most pronounced. With as few as 13 stages, profound errors in second-generation sizes and spatial distributions are avoided (Fig. 4C; 5A, E). As processor speeds increase, even finer-stage resolutions may be used, provided the time step may be made small enough to ensure stability. In any case, the MUSCL will be equally effective in minimizing numerical diffusion in the age domain without a significant increase in run time. This will also be an advantage, as increases in knowledge of any given species render the biological model more complex and calculation intensive.

Implementation of the MUSCL is fairly straightforward and

requires only 10–20 additional lines in the reaction term calculation. The time required to execute these lines is small relative to the reaction term. In contrast, a 3- to 5-fold increase in the number of state variables essentially requires a 3- to 5-fold increase in the number of times the reaction term is calculated, plus as many additional calculations of advection and diffusion. The implementation is also highly modular, from both a programming and a theoretical point of view. It requires no change in the underlying model and is robust to changes in the physical or biological model. The level of detail in the age distribution may be easily tuned without affecting the underlying model, and other processes, such as stochastic models or species behaviors and interactions, may be added easily.

Assessment of a numerical scheme should, at minimum, contain the following: (1) a simplified case for which the analytical solution is known, and (2) a model run with full complexity, where effectiveness is examined in many different domains. Software engineering and scheme implementation should also be considered, as some numerical schemes may be accompanied by costs such as run time or restrictions on other aspects of the model. The assessment shown here highlights a few key ways of analyzing the output, with emphasis on early adulthood and egg production. A more thorough assessment may be prudent depending on the particular goals of the modeling exercise.

References

- Ayati, B. P. 2000. A variable time step method for an age-dependent population model with nonlinear diffusion. *SIAM J. Numer. Anal.* 37(5):1571-1589.
- Batchelder, H. P., C. A. Edwards, and T. M. Powell. 2002. Individual-based models of copepod populations in coastal

- upwelling regions: implications of physiologically and environmentally influenced diel vertical migration on demographic success and nearshore retention. *Prog. Oceanogr.* 53:307-333.
- Belehradek, J. 1935. Temperature and living matter. *Proto-plasma Monogr.* 8:1-277.
- Campbell, R. G., M. W. Wagner, G. J. Teegarden, C. A. Boudreau, and E. G. Durbin. 2001. Growth and development of the copepod *Calanus finmarchicus* reared in the laboratory. *Mar. Ecol. Prog. Ser.* 221:161-183.
- Carlotti, F., and K.-U. Wolf. 1998. A Lagrangian ensemble model of *Calanus finmarchicus* coupled with a 1-D ecosystem model. *Fish. Ocean.* 7:191-204.
- Davis, C. S. 1984. Interaction of a copepod population with the mean circulation on Georges Bank. *J. Mar. Res.* 42:573-590.
- de Roos, A. M. 1988. Numerical methods for structured population models: the Escalator Boxcar Train. *Numerical Methods for Partial Differential Equations.* 4(3):173-195.
- de Roos, A. M., and J. A. J. Metz. 1991. Towards a numerical analysis of the Escalator Boxcar Train. *In* J.A. Goldstein, F. Kappel, W. Schappacher [eds], *Differential Equations with Applications in Biology, Physics and Engineering.* Lect. Notes in Pure and Appl. Math. 133:91-113, Marcel Dekker, New York.
- de Roos, A. M., O. Diekmann, J. A. J. Metz. 1992. Studying the dynamics of structured population models: a versatile technique and its application to *Daphnia*. *Am. Nat.* 139(1):123-147.
- Durbin, E. G., R. G. Campbell, M. C. Casas, M. D. Ohman, B. Niehoff, J. Runge, and M. Wagner. 2003. Interannual variation in phytoplankton blooms and zooplankton productivity and abundance in the Gulf of Maine during winter. *Mar. Ecol. Prog. Ser.* 254:81-100.
- Durrant, D. R. 1999. *Numerical Methods for Wave Equations in Geophysical Fluid Dynamics.* Springer-Verlag, New York.
- Eiane, K., D. L. Aksnes, M. D. Ohman, S. Wood, and M. B. Martinusse. 2002. Stage specific mortality of *Calanus* spp. under different predation regimes. *Limnol. Oceanogr.* 47:636-645.
- Feldman, G. C., and C. R. McClain. 2007. Ocean Color Web, SeaWiFS Reprocessing 5.1 and MODIS-Aqua Reprocessing 1.1. NASA Goddard Space Flight Center. Eds. Kuring, N., Bailey, S. W, <http://oceancolor.gsfc.nasa.gov/>
- Gentleman, W. 2002. A chronology of plankton dynamics in silico: how computer models have been used to study marine ecosystems. *Hydrobiologia* 480:69-85.
- Gentleman, W., A. Leising, B. Frost, S. Strom, and J. Murray. 2003. Functional responses for zooplankton feeding on multiple resources: a review of assumptions and biological dynamics. *Deep-Sea Res. II* 50:2847-2875.
- Gurney, W. S. C., D. C. Speirs, S. N. Wood, E. D. Clarke, and M. R. Heath. 2001. Simulating spatially and physiologically structured populations. *J. Anim. Ecol.* 70:881-894.
- Hu, Q., C. S. Davis, C. M. Petrik. 2008. A simplified age-stage model for copepod population dynamics. *Mar. Ecol. Prog. Ser.* 360:179-187.
- Löhner, R. 2001. *Applied Computational Fluid Dynamics Techniques: An Introduction Based on Finite Element Methods.* John Wiley and Sons, Chichester, UK.
- Lynch, E., W. C. Gentleman, D. J. McGillicuddy Jr, and C. S. Davis. 1998. Biological/physical simulations of *Calanus finmarchicus* population dynamics in the Gulf of Maine. *Mar. Ecol. Prog. Ser.* 169:189-210.
- Mauchline, J. 1998. *The Biology of Calanoid Copepods.* Academic Press, San Diego.
- Naimie, C. E. 1996. Georges Bank residual circulation during weak and strong stratification periods: prognostic numerical model results. *J. Geophys. Res.* 101:6469-6486.
- Odman, M. T. 1997. A quantitative analysis of numerical diffusion introduced by advection algorithms in air quality models. *Atmos. Environ.* 31(13):1933-1940.
- Rinke, K., and J. Vijverberg. 2005. A model approach to evaluate the effect of temperature and food concentration on individual life-history and population dynamics of *Daphnia*. *Ecol. Modeling* 186:326-344.
- Runge, J. A., P. J. S. Franks, W. C. Gentleman, B. A. Megrey, K. A. Rose, F. E. Werner, and B. Zakardjian. 2004. Diagnosis and prediction of variability in secondary production and fish recruitment processes: developments in physical-biological modeling. *In*: A. R. Robinson and K. Brink [eds], *The Sea, Vol. 13: The Global Coastal Ocean: Multi-Scale Interdisciplinary Processes.* Harvard Univ. Press, Cambridge, MA.
- Speirs, D. C., W. S. C. Gurney, M. R. Heath, W. Horbelt, S. N. Wood, and B. A. de Cuevas. 2006. Ocean-scale modeling of the distribution, abundance, and seasonal dynamics of the copepod *Calanus finmarchicus*. *Mar. Ecol. Prog. Ser.* 313:173-192.
- van Leer, B. 1979. Towards the ultimate conservative difference scheme, V. A second order sequel to Godunov's method. *J. Com. Phys.* 32:101-136.
- Wang, Y., and K. Hutter. 2001. Comparisons of numerical methods with respect to convectively dominated problems. *Int. J. Numer. Meth. Fluids* 37:721-745.
- Wroblewski, J. S. 1982. Interaction of currents and vertical migration in maintaining *Calanus marshallae* in the Oregon upwelling zone: a simulation. *Deep Sea Res. Part A* 29:665-686.
- Zakardjian, B. A., J. Sheng, J. A. Runge, I. McLaren, S. Plourde, K. R. Thompson, and Y. Gratton. 2003. Effects of temperature and circulation on the population dynamics of *Calanus finmarchicus* in the Gulf of St. Lawrence and Scotian Shelf: study with a coupled, three-dimensional hydrodynamic, stage-based life history model. *J. Geophys. Res.* 108(C11):GLO 17-1.

Submitted 14 November 2007

Revised 22 April 2008

Accepted 30 June 2008